Monthly Notices
of the
ROYAL ASTRONOMICAL SOCIETY

MNRAS **470,** 4222–4230 (2017)
Advance Access publication 2017 June 12

doi:10.1093/mnras/stx1461

Laboratory study of methyl isocyanate ices under astrophysical conditions

B. Maté,[1⋆] G. Molpeceres,[1] V. Timón,[1] I. Tanarro,[1⋆] R. Escribano,[1] J. C. Guillemin,[2] J. Cernicharo[3] and V. J. Herrero[1⋆]

[1]*Instituto de Estructura de la Materia (IEM-CSIC), Serrano 121-123, E-28006 Madrid, Spain*
[2]*Institut des Sciences Chimiques de Rennes, École Nationale Supérieure de Chimie de Rennes, CNRS, UMR 6226, 11 Allée de Beaulieu, CS 50837, F-35708 Rennes Cedex 7, France*
[3]*ICMM-CSIC, Molecular Astrophysics Group, c./Sor Juana Inés de la Cruz 3, Cantoblanco, E-28049 Madrid, Spain*

Accepted 2017 June 8. Received 2017 June 8; in original form 2017 May 12

ABSTRACT

Methyl isocyanate has been recently detected in comet 67P/Churyumov–Gerasimenko (67P/CG) and in the interstellar medium. New physicochemical studies on this species are now necessary as tools for subsequent studies in astrophysics. In this work, infrared spectra of solid CH_3NCO have been obtained at temperatures of relevance for astronomical environments. The spectra are dominated by a strong, characteristic multiplet feature at 2350–2250 cm^{-1}, which can be attributed to the asymmetric stretching of the NCO group. A phase transition from amorphous to crystalline methyl isocyanate is observed at ∼90 K. The band strengths for the absorptions of CH_3NCO in ice at 20 K have been measured. Deuterated methyl isocyanate is used to help with the spectral assignment. No X-ray structure has been reported for crystalline CH_3NCO. Here we advance a tentative theoretical structure, based on density functional theory (DFT) calculations, derived taking the crystal of isocyanic acid as a starting point. A harmonic theoretical spectrum is then calculated for the proposed structure and compared with the experimental data. A mixed ice of H_2O and CH_3NCO was formed by simultaneous deposition of water and methyl isocyanate at 20 K. The absence of new spectral features indicates that methyl isocyanate and water do not react appreciably at 20 K, but form a stable mixture. The high CH_3NCO/H_2O ratio reported for comet 67P/CG, and the characteristic structure of the 2350–2250 cm^{-1} band, makes it a very good candidate for future astronomical searches.

Key words: methods: laboratory: solid state – techniques: spectroscopic – ISM: clouds – infrared: ISM.

1 INTRODUCTION

Organic isocyanates (R-NCO) have been synthesized since the mid-nineteenth century and their chemistry has been extensively investigated due to their technical applications in the production of polyurethane and polyureas, in the industry of chemical pesticides, and in the preparation of diverse bio-compounds (Saunders & Slocombe 1948; Ozaki 1972). Methyl isocyanate (CH_3NCO), the first term in the alkyl isocyanate series, came to notoriety in 1984 when it was identified as the main toxic agent responsible for the Bhopal massive poisoning (D'Silva et al. 1986), which is generally regarded as the worst industrial catastrophe to date. Very recently, methyl isocyanate has been detected at the surface of comet 67P/Churyumov–Gerasimenko (CG) (Goesmann et al. 2015) and in the interstellar medium (ISM) (Halfen, Ilyushin & Ziurys 2015; Cernicharo et al. 2016).

⋆E-mail: belen.mate@csic.es (BM); i.tanarro@csic.es (IT); v.herrero@csic.es (VJH)

Electron diffraction (Eyster, Gillette & Brockway 1940; Anderson, Rankin & Robertson 1972), microwave (MW) spectra (Curl et al. 1963; Lett & Flygare 1967; Koput 1984; Koput 1986; Kasten & Dreizler 1986) and theoretical calculations (Koput 1988; Sullivan et al. 1994; Zhou & Durig 2009; Reva, Lapinski & Fausto 2010; Dalbouha et al. 2016) indicate that the CH_3NCO molecule is an asymmetric top with a CNC angle of about 140° and a small barrier (≈20–30 cm^{-1}) for the torsion of the methyl group. Its large amplitude internal motions (CH_3 torsion and CNC bend) complicate the spectral analysis, and although the high accuracy of the available experimental data (Cernicharo et al. 2016) has allowed the detection of this molecule in the gas phase of the ISM, an appreciable discrepancy persists in the value of the *A* rotational constant (Halfen, Ilyushin & Ziurys 2015; Cernicharo et al. 2016; Dalbohua et al. 2016).

Possible gas-phase mechanisms for the production of CH_3NCO in the ISM have been advanced in the literature (Halfen, Ilyushin & Ziurys 2015), but it is more likely that this comparatively 'complex' molecule (Herbst & van Dishoeck 2009) has been formed through solid phase chemistry (Goesmann et al. 2015) at the surface or in

the bulk of ice mantles in cold astronomical media and then released to the gas phase in the transition to higher temperature conditions (Cernicharo et al. 2016). The possibility of detecting methyl isocyanate in astronomical ices is thus enticing. In fact, the first detection of the compound in space was reported for solid material from the surface of comet 67P/CG as a part of the Rosetta mission. It was based on mass spectrometric measurements performed by the COSAC instrument on board the Philae lander (Goesmann et al. 2015). This circumstance was however exceptional and future searches for the molecule in astronomical ices will require infrared (IR) spectroscopy.

Experimental IR and Raman spectra have also been reported for a variety of methyl isocyanate samples (Hirschmann, Kniseley & Fassel 1965; D´Hendecourt & Allamandola 1986; Sullivan et al. 1994; Zhou & Durig 2009; Reva, Lapinski & Fausto 2010). The mid-IR absorption spectrum is dominated by a very prominent band at about 2350–2250 cm^{-1} attributed to the asymmetric stretching of the NCO group. Other bands appear at 3000–2950 cm^{-1} (CH_3 stretchings), 1460–1420 cm^{-1} (NCO symmetric stretch and CH_3 deformations), 1150–1130 cm^{-1} (CH_3 rocking vibration), 870–850 cm^{-1} (C–N stretching) and 625–580 cm^{-1} (NCO bendings). The bands of the large amplitude motions appear at lower frequencies, 190–170 cm^{-1} for the CNC in-plane bending and 20–30 cm^{-1} for the CH_3 torsion, and have been determined from far IR, Raman and MW spectra (Koput 1986; Sullivan et al. 1994). In spite of their low frequencies, these bands could also have some influence on the mid-IR region through combinations with higher frequency modes (Zhou & Durig 2009; Reva, Lapinski & Fausto 2010; Dalbouha et al. 2016).

Most previous studies, especially the theoretical calculations, have focused on the determination of the structure and spectra of the isolated CH_3NCO molecule. IR spectra of liquid and solid methyl isocyanate have also been measured, but they were basically used for a global spectral assignment of vibrational bands. In this work, we study the evolution of the IR spectra of solid CH_3NCO over the wide temperature range of relevance to astronomical environments. The IR spectrum of CD_3NCO has been added as a supplement for the analysis of the spectrum of CH_3NCO. We also report the spectrum of CH_3NCO diluted in water ice at 20 K, a temperature typical for interstellar cold clouds, and we discuss the phase transition from amorphous to crystalline, at ∼90 K. As part of the study we advance a tentative theoretical structure for crystalline CH_3NCO, based on density functional theory (DFT) calculations, and provide an estimate of the IR band strengths of CH_3NCO in ice that might be of help for future astronomical searches.

2 EXPERIMENTAL

The synthesis of Han, Pearson & Baillie (1989) was modified to prepare methyl isocyanate (CH_3NCO) and fully deuterated methyl isocyanate (CD_3NCO). Silver cyanate (15.0 g, 0.1 mol), dry diethyleneglycol dibutyl ether (25 mL) and iodomethane (7.10 g, 50 mmol) or iodomethane-d_3 (7.25 g, 50 mmol) were mixed together in a cell equipped with a magnetic stirring bar and a stopcock. The cell was immersed in a liquid nitrogen bath and degassed. The mixture was heated under stirring at 90°C for 20 h. The cell was then fitted on a vacuum line (0.1 mbar) equipped with two traps and low boiling compounds were distilled. The first trap was immersed in a bath cooled at −30°C to remove high boiling compounds. The low boiling methyl isocyanate was selectively condensed in the second trap immersed in a liquid nitrogen bath. Yield: 40 per cent. The deuterated species was characterized by ^{13}C NMR spectroscopy:

CD_3NCO: ^{13}C NMR ($CDCl_3$, 100 MHz) δ 27.4 (sept., $^1J_{CD}$ = 21.7 Hz, CD_3), 121.4 (s brd, NCO). (**Caution!** Methyl isocyanate is a highly toxic, severe lachrymatory agent and should be handled with care.)

The set-up for infrared spectroscopy of ices has been described in detail in previous publications (Maté et al. 2003; Gálvez et al. 2008; Maté et al. 2014) and only the details relevant to the present investigation are given here. It consists of a vacuum chamber with a closed-cycle He cryostat, coupled to a Fourier transform infrared spectroscopy (FTIR) spectrometer. Inside the chamber, solid layers of methyl isocyanate were deposited from the vapour phase on an IR transparent Si substrate in contact with the head of the cryostat. The CH_3NCO and CD_3NCO vapours were introduced by means of a needle valve connecting the chamber with a small pyrex flask containing approximately 5 ml of liquid methyl isocyanate. For a better handling of the vapor flow to the chamber, the flask was held in an ice bath or in a bath with ice and salt. The liquid samples were subjected to three freeze–pump–thaw cycles for degassing before allowing methyl isocyanate into the vacuum chamber. Deposits were formed at substrate temperatures of 20 and 110 K. Deposition pressures in the $\approx 10^{-6}$ mbar range and deposition times of several minutes were typically used. Normal incidence transmission spectra were recorded with a Bruker Vertex 70 FTIR spectrometer coupled to the vacuum chamber through two KBr windows. The spectra were recorded with a resolution of 2 cm^{-1} using an HgCdTe (MCT) detector refrigerated with liquid nitrogen.

Absolute gas-phase densities in the deposition chamber were estimated with the help of a calibrated quadrupole mass spectrometer (QMS) placed in a differentially pumped adjacent vacuum chamber and connected to the deposition chamber by a regulation valve. The calibration of the QMS is described in the Appendix.

3 THEORETICAL CALCULATIONS

As far as we know, no X-ray structure has been reported for crystalline CH_3NCO. In this work, we derive a tentative structure taking the crystal of isocyanic acid as a starting point (von Dohlen & Carpenter 1955). A similar strategy was successfully applied to the study of the structure of schwertmannite (Fernández-Martínez et al. 2010), where a theoretical unit cell based on that of the chemically related akageneite was successfully used for the interpretation of the X-ray data.

In this work, H atoms in the unit cell of isocyanic acid were substituted by CH_3 groups, and the new unit cell was optimized using the CASTEP code (Clark et al. 2005; Refson, Tulip & Clark 2006), a DFT plane wave pseudopotential method. At the minimum in the potential energy surface, atomic forces and charges were evaluated to predict the harmonic vibrational spectrum. For the optimization process with CASTEP, the generalized gradient approximation (GGA) was chosen with the PBE exchange-correlation functional (Perdew, Burke & Ernzerhof 1996). The Grimme DFT-D2 correction (Grimme 2006) was also applied. The convergence criteria were set at 1×10^{-5} eV $atom^{-1}$ for the energy, 0.02 eV $Å^{-1}$ for the interatomic forces, 830 eV for the cut-off energy, maximum stress 0.05 GPa and 0.001 Å for the displacements.

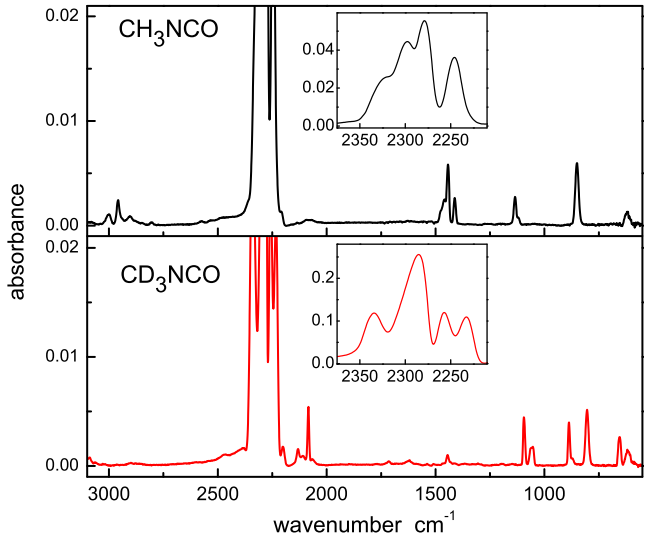

Figure 1. Mid-IR spectra of solid methyl isocyanate and fully deuterated methyl isocyanate deposited at 20 K from the vapour phase.

Table 1. Observed IR absorption wavenumbers (cm^{-1}) and assignment of the spectrum of amorphous methyl isocyanate (vapour deposited at 20 K). Symbols ν, δ, β and r stand for stretch, deformation, bending and rocking vibrations, respectively.

CH_3NCO	CD_3NCO	Assignment
3000	–	ν_a-CH_3
2958	–	ν_s-CH_3
2327, 2298, **2278**, 2246	2335, **2285**, 2258, 2233	ν_a-NCO
–	2132	ν_a-CD_3
–	2085	ν_s-CD_3
1456	–	δ_a-CH_3
1443	1444	ν_s-NCO
1412	–	δ_s-CH_3
1135	–	r-CH_3
–	1094	δ_a-CD_3
–	1056	δ_s-CD_3
–	887	r-CD_3
850	802	ν-CN
616	616	β-NCO

Note. Subindices a and s denote asymmetric and symmetric modes, respectively. The wavenumber of the maximum peak within the ν_a-NCO band is given in bold.

4 RESULTS AND DISCUSSION

4.1 Infrared spectra and phase transition

Mid-IR spectra of CH_3NCO and CD_3NCO solid samples formed by vapour deposition at 20 K are shown in Fig. 1. At this temperature, which is typical for the grain mantles in interstellar dense clouds, amorphous solids are formed. The spectra are dominated by an intense band, with a quadruplet structure between 2360 and 2200 cm^{-1}, as shown in the insets of Fig. 1, which corresponds to the asymmetric stretching vibration of the NCO group, ν_a-NCO. The band roughly spans the same wavenumber region for the two isotopic variants, but the internal structure of the band and relative intensity of the maxima are isotope dependent.

The assignment of all normal mode vibrations observed in the 3100–550 cm^{-1} range is given in Table 1. Minor features, not listed in the table, can also be discerned in the spectra. They are likely due to overtones or combination bands. We are only aware of a previous mid-IR spectrum of amorphous CH_3NCO reported by D'Hendecourt & Allamandolla (1986), but in this spectrum the most intense band was saturated. The rest of the bands are in good agreement with those of Fig. 1. A vibrational spectrum of CD_3NCO is presented here for the first time.

The assignment of the three peaks between 1456 and 1412 cm^{-1} in CH_3NCO is not unanimous and they are sometimes interchanged in the literature (Sullivan et al. 1994; Zhou & Durig 2009; Reva, Lapinski & Fausto 2010). DFT calculations of the molecular spectrum show that the ν_s-NCO vibration is largely mixed with bending CH_3 motions (Reva, Lapinski & Fausto 2010). In any case, the contribution of the symmetric NCO stretch to the overall absorption in this frequency interval is small as clearly seen in the spectrum of CD_3NCO, where methyl bending modes are redshifted upon deuterium substitution and only a small peak corresponding to ν_s(NCO) is left at 1444 cm^{-1}.

In the amorphous solids, the components of the ν_a-NCO band are not resolved. For CH_3NCO, a similar band pattern, albeit with full resolution of the four band peaks, is observed in the matrix experiments of Reva, Lapinski & Fausto (2010), carried out at temperatures between 8 and 20 K. The band is perturbed by interaction with lower frequency modes. The splitting in multiple peaks has been attributed to a coupling of the NCO asymmetric stretch with the torsion of the methyl group (Reva, Lapinski & Fausto 2010). In addition, second-order perturbation theory calculations (Dalbouha et al. 2016; Senent 2017) show that the band maximum is redshifted by more than 10 cm^{-1} with respect to the harmonic value due to a Fermi resonance with the δ_a-CH_3 + ν-CN combination band. Both the Fermi resonance and the torsion of the methyl group are affected by the H/D substitution, which might explain the change in the band profile between CH_3NCO and CD_3NCO observed in the insets of Fig. 1.

Experimental band strengths for CH_3NCO can be useful for astronomical observations and are listed in Table 2. They were determined using the expression

$$A'_i = \frac{1}{N_{\rm CH3NCO}} \int_i \tau\,(\nu)\,{\rm d}\nu \qquad (1)$$

where A'_i is the strength of band i, $N_{\rm CH3NCO}$ is the column density of methyl isocyanate and the integral of the optical depth is obtained from the measured integrated absorbance (absorbance $= \tau(\nu)/\ln 10$) over the frequency range of band i. The column density of CH_3NCO was obtained using the measured gas-phase density (see Section 2) and assuming a sticking probability of one for deposition at 20 K:

$$N_{\rm CH3NCO} = n_{\rm CH3NCO} \left(\frac{kT}{2\pi m}\right)^{1/2} \Delta t \qquad (2)$$

where $n_{\rm CH3NCO}$ is the molecular density of gas-phase methyl isocyanate in the chamber, which was kept constant during deposition, and all other parameters were defined above.

The band strengths estimated from the measured spectra using equation (1) are termed 'apparent', as opposed to 'absolute', which are derived from optical constants (see for instance Hudson, Ferrante & Moore 2014). Apparent band strengths include losses due to reflection and interference that can be substantial for thin ice samples. For the typical thickness of the present samples ($\approx$150 μm) these effects are expected to be small. As the experimental error of the magnitudes is derived, the main uncertainty in the integral of equation (1) is the subtraction of the baseline which is estimated to be $\approx$5 per cent for the ν_a-NCO band and up to $\approx$20 per cent for the

Table 2. Experimental band strengths for the observed absorptions of CH_3NCO.

Peak (cm^{-1})	Wavenumber range (cm^{-1})	Wavelength range (μm)	A' (cm molecule^{-1})	Band assignment
3000	3035–2979	3.29–3.36	8.8×10^{-19}	ν_a-CH_3
2958	2977–2930	3.36–3.41	1.4×10^{-18}	ν_s-CH_3
2278	2432–2160	4.11–4.63	1.3×10^{-16}	ν_a-NCO
1443	1492–1427	6.70–7.01	4.9×10^{-18}	δ_a-CH_3 + ν_s-NCO
1412	1428–1396	7.04–7.16	1.2×10^{-18}	δ_s-CH_3
1135	1076–1100	9.29–9.09	1.8×10^{-18}	r-CH_3
850	880–820	11.36–12.19	4.6×10^{-18}	ν-CN
616	670–550	14.92–18.18	1.4×10^{-18}	β-NCO

Note. The uncertainty in the value of the ν_a-NCO band is of the order of 30 per cent mostly due to the inaccuracy in the estimate of the column density. For the weakest bands, the uncertainty may be 40 per cent.

weakest peaks. The error in the value of the column density is of the order of 30 per cent and is due to the uncertainty in the gas-phase density of CH_3NCO during deposition (see the Appendix). Consequently, the uncertainties in the estimated band strengths are in the 30–40 per cent range.

The most intense band (ν_a-NCO) has a strength comparable to that reported for the same vibration in solid isocyanic acid at 145 K (1.6×10^{-16} cm molecule^{-1}) by Lowenthal, Khanna & Moore (2002) and is of the order of other stretching vibrations of common ice components (CO, CO_2, CH_3OH, ...) (Gerakines et al. 1995; Bouilloud et al. 2015). D'Hendecourt & Allamandola (1986) reported an IR spectrum for pure solid CH_3NCO at 10 K. In their measurements, the ν_a-NCO band was saturated and they could only provide a lower limit of 10^{-16} cm molecule^{-1} for the band strength, which is consistent with the present determination. In addition, they gave a value of 7.5×10^{-18} cm molecule^{-1} for the band at 2958 cm^{-1} and 2.8×10^{-18} cm molecule^{-1} for the band at 1135 cm^{-1}, which they attributed to a CO stretching vibration, but noted that these values were very uncertain. The latter value is in reasonable agreement with our result, but that for the 2958 cm^{-1} band is too large. We believe that there might be a mistake in the value reported by D'Hendecourt & Allamandola (1986) for this band strength since in their experimental spectrum (and in that of the present work) the two bands have comparable intensities.

The spectra of the solid deposits hardly change with rising temperature over the 20–85 K range, but heating to ≈90 K leads to appreciable variations in the band shapes and shifts in the absorption maxima. Overall the peaks become sharper and in many cases split or grow shoulders, as exemplified in Fig. 2 for the ν_a-NCO band. These changes are indicative of sample crystallization and are due to the growing order and geometric restrictions for the molecules in a crystalline frame, which result in different environments for a given functional group. Above this temperature, the spectra remain stable until sublimation that takes place at about 130 K.

The stability of the CH_3NCO spectra in the 20–85 K range questions the qualitative model of Reva, Lapinski & Fausto (2010) in which the quadruplet structure of the band is attributed to a coupling of stretching and torsional modes. The model interprets the band profile in terms of transitions from the ground state and the first state of the CH_3 torsion to $v = 1$ of ν_a-NCO and $v = 0$, 1 and 2 of the torsion. The first torsional level, at ≈20–30 cm^{-1} (Reva, Lapinski & Fausto 2010), must be appreciably populated even at 20 K. When the temperature is increased from 20 to 85 K, the population distribution of the torsional levels should change noticeably, leading to significant variations in the band contour which are not observed. In spite of this shortcoming of the model, some coupling of

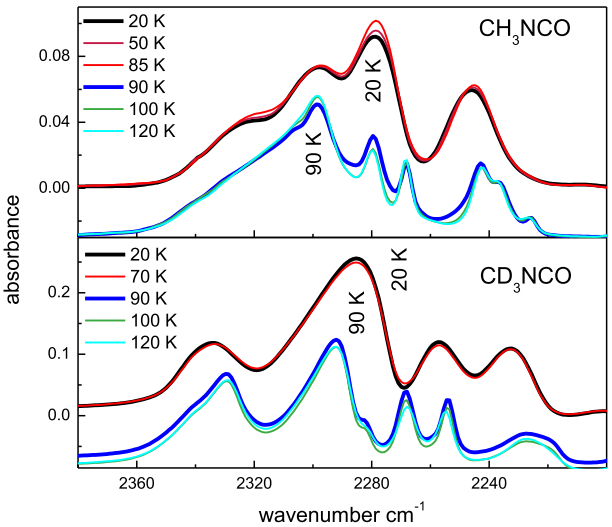

Figure 2. Evolution of the ν_{as}-NCO band with temperature for the 20 K solid deposits of CH_3NCO and CD_3NCO. A shift downward of −0.03 and −0.08 is introduced in the absorbance axis of the spectra taken in the range 90–120 K for CH_3NCO and CD_3NCO, respectively, for a better visualization. Note the splitting of the third peak in order of decreasing wavenumber.

stretching with torsional modes remains a plausible explanation for the quadruplet, especially considering that the experimental ν_a-NCO band of HNCO has just one peak (Teles et al. 1989; Lowenthal, Khanna & Moore 2002) and that the estimated spacing between torsional levels is roughly comparable to the separation between the observed band peaks (Reva, Lapinski & Fausto 2010).

For crystalline CD_3NCO, the location of the band maximum does not change much with respect to the amorphous sample (see the lower panel of Fig. 2), but for crystalline CH_3NCO (upper panel), the maximum appears at 2300 cm^{-1}, more than 20 cm^{-1} higher than the maximum of the amorphous solid (see Table 1). The different band profiles and specifically the frequency shift of the maximum should be considered in possible searches for frozen methyl isocyanate in astronomical environments above or below ≈90 K.

4.2 Theoretical model of crystalline CH_3NCO

The starting point for a tentative crystalline structure for CH_3NCO was the unit cell of isocyanic acid. X-ray measurements have shown that HNCO has four molecules and orthorhombic symmetry

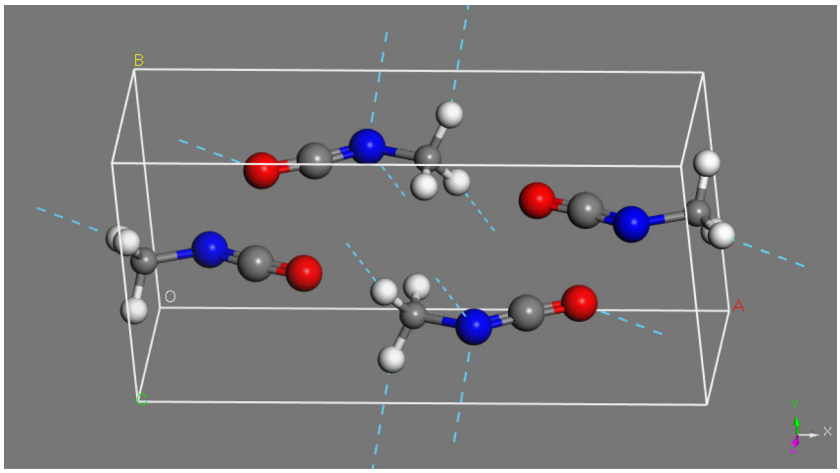

Figure 3. Tentative structure of the unit cell of methyl isocyanate. Dashed lines indicate hydrogen bonds.

Table 3. Experimental unit cell parameters of isocyanic acid and calculated values for isocyanic acid and methyl isocyanate.

Unit cell dimentions	HNCO X-ray, ref. (doh55)	HNCO This work (DFT)	CH_3NCO This work (DFT)
a (Å)	10.82	10.93	12.57
b (Å)	5.23	5.05	6.26
c (Å)	3.57	3.57	3.63
α (deg)	90	90	90
β (deg)	90	90	89.52
γ (deg)	90	90	90
V (Å^3)	202.02	197.06	286.12

(von Dohlen & Carpenter 1955). As a check of consistency, the observed structure of isocyanic acid itself was first relaxed. Table 3 compares the cell parameters of the DFT optimized structure for HNCO with those obtained from the X-ray data.

The calculations reproduce the HNCO cell dimensions within 2 per cent and maintain the orthorhombic crystal structure. The crystallographic data yield N. . . .N distances of 3.07 Å and N. . . .C–N angles of 120.6°, which are suggestive of the presence of N–H. . . .N hydrogen bonds. Very similar values (3.01 Å and 119.7°, respectively) are obtained in the present calculations, which confirm the existence of N. . . .H hydrogen bonds, for which a bond length of 1.89 Å is predicted. The calculations also corroborate the conclusion of the X-ray work on the absence of H. . . .O hydrogen bonds that are precluded by geometrical constraints.

The H atoms in the isocyanic molecules were then substituted by methyl groups, and the structure was relaxed. The optimized values for the unit cell of methyl isocyanate are also listed in Table 2. The crystal is monoclinic, but very close to orthorhombic, since only one angle ($\beta = 89.52°$) deviates slightly from 90°. The cell volume is increased as expected due to the inclusion of CH_3 groups. Two types of hydrogen bonds are identified in the modelled CH_3NCO crystal: (1) a C–H. . . .O bond with an H. . . .O distance of 2.43 Å and a C–H. . . .O angle of 157° and (2) a weaker C–H. . . .N bond with an H. . . .N distance of 2.66 Å and a C–H. . . .N angle of 160°. The predicted structure is displayed in Fig. 3. Hydrogen bonds in this figure are represented by dashed lines. The zigzag ordering of the NCO units, observed in the original HNCO crystal (von Dohlen & Carpenter 1955), is maintained in CH_3NCO.

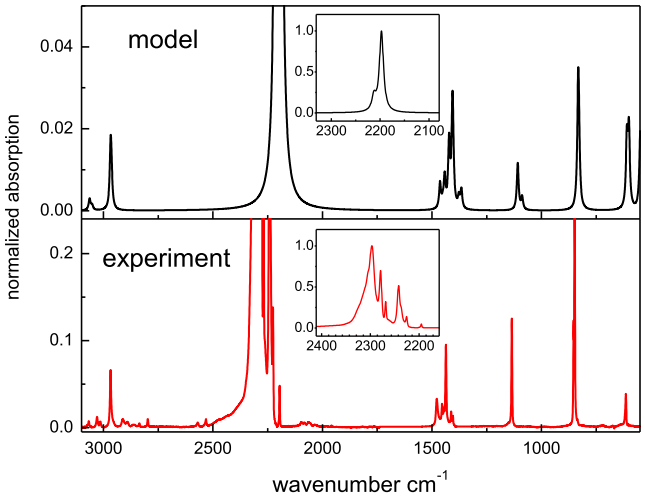

Figure 4. Comparison of calculated (upper panel) and experimental (lower panel) spectra for crystalline CH_3NCO. Both spectra are normalized to one at their maximum peaks (see the inset). Note the differences in the vertical scales for the weaker absorptions.

A harmonic theoretical spectrum was calculated for the proposed structure. The unit cell of the crystal has 81 vibrational normal modes, which in the mid-IR mainly correspond to combinations of vibrations of functional groups of the individual molecules. Many of these modes are infrared inactive because the corresponding molecular vibrations cancel each other by symmetry and do not give rise to a net change of the dipole moment in the cell. In Table 4, the modes active within a given wavelength interval are grouped and assigned. Calculated band strengths are also listed. The band strength is obtained by adding the strengths of the individual modes in the interval of interest; this value is then divided by four to account for the number of molecules in the unit cell. The approximate assignment gives the predominant vibration for the interval considered. In many cases, more than one type of molecular vibration contributes to a given mode. There is no single mode of the crystal that contains the ν_s-NCO vibration alone; it appears always mixed with CH_3 deformations. Note that this vibration was observed to be weak and also mixed with CH_3 deformations in the amorphous solid (see above) and in the isolated molecule (Reva, Lapinski & Fausto 2010).

Table 4 Assignment and band strengths of the theoretical IR spectrum of crystalline methyl isocyanate in the 3100–500 cm^{-1} range.

Wavenumber range (cm^{-1})	Assignment	Band strength (cm $molecule^{-1}$)
3080–3020	ν_a-CH_3	1.45×10^{-18}
2987–2933	ν_s-CH_3	5.55×10^{-18}
2327–2066	ν_a-NCO	2.74×10^{-16}
1480–1340	δ_s-CH_3 + ν_s-NCO + (ν_a-NCO)	1.60×10^{-17}
1107–1074	r-CH_3	3.52×10^{-18}
870–791	ν-CN	1.00×10^{-18}
663–569	β-NCO	1.09×10^{-17}
570–508	β-NCO	5.18×10^{-18}

Note. The assignments are approximate and correspond to the predominant vibrations in the indicated wavenumber intervals.

The calculated band strengths for the theoretical crystal are roughly a factor of two larger than the experimental band strengths for the amorphous solid. This result may be considered acceptable, keeping in mind that the theoretical structure is just a prediction, the approximations involved in the theoretical model and the uncertainty in the experimental measurements. The theoretical spectrum is compared in Fig. 4 with an experimental spectrum of crystalline CH_3NCO obtained by vapour deposition at 110 K.

For the comparison, the calculated vibrational modes have been represented by Gaussian functions of 10 cm^{-1} full width at half-maximum and the two spectra have been normalized to one at their highest peaks (see insets in Fig. 4). The calculations reproduce reasonably well the pattern of weaker absorptions over the 3100–700 cm^{-1} range and partly account for the structure observed around 3000 and 1400 cm^{-1} due to CH_3 stretchings and deformations, respectively. However, the intensities of these absorptions with respect to the strongest peak in the spectrum are too weak as compared to the experimental ones.

The dominant theoretical band is in worse agreement with the experiment. The theoretical peak is calculated at 2174 cm^{-1} whereas the experimental one is found at 2300 cm^{-1}, and the multiplet structure of the measured band is also not reproduced in the calculations. The discrepancy is hardly surprising since, in addition to the very approximate nature of the proposed crystal structure, the harmonic model used for the calculation of the spectra is not expected to account for the strong perturbations of this band, already commented on in the discussion of the amorphous solid spectra. The fact that the theoretical ν_a-NCO band intensity appears concentrated in a single peak explains, at least partially, the lower relative intensities of the rest of the theoretical bands shown in Fig. 4.

4.3 Methyl isocyanate in water ice

The spectrum of a mixture of H_2O and CH_3NCO ice is displayed in Fig. 5. The mixed ice was formed by simultaneous deposition of water and methyl isocyanate at 20 K. The CH_3NCO/H_2O molecular ratio in the gas phase was ≈2.7 per cent. At this deposition temperature, the sticking coefficient should be nearly one for the two species and, considering that the collision frequency of molecules of mass m_i with the substrate surface is proportional to $m_i^{-0.5}$, the ratio of CH_3NCO molecules in the mixed ice is estimated to be ≈1.5 per cent, which is close to the CH_3NCO/H_2O proportion (1.3 per cent) found in the material excavated by the COSAC instrument at the surface of comet 67P/CG.

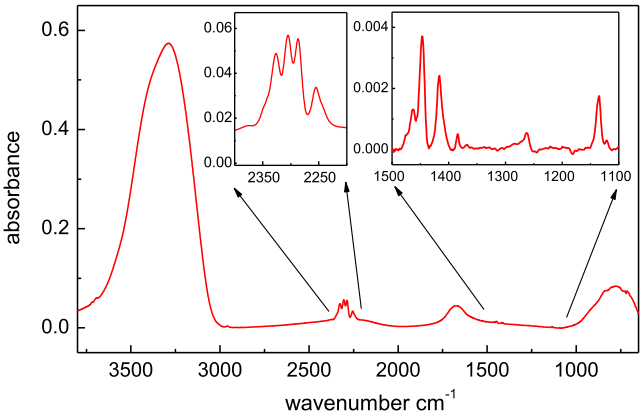

Figure 5. Spectrum of a mixture of H_2O and CH_3NCO. The molecular ratio of methyl isocyanate is ≈1.5 per cent (see the text). Insets show enlargements of the 2200–2400 and 1100–1500 cm^{-1} intervals.

Table 5. Wavenumbers of the four maxima in the ν_a-NCO band of CH_3NCO in various environments.

ν_a-NCO cm^{-1} amorph. solid, 20 K, this work	ν_{as} (NCO) cm^{-1} H_2O ice, 20 K, this work	ν_{as} (NCO) cm^{-1} N_2 matrix, 8 K, ref. (rev10)	ν_{as} (NCO) cm^{-1} vapour ref. (sul94)
2327	2336	2334.7	2340
2298	2305	2307.9	2308
2279	2286	2288.9	2285
2246	2255	2259.7	2265

The spectrum is dominated by the intense, broad OH stretching, ν(OH), band of water at 3288 cm^{-1}. Typical water absorptions corresponding to bending ($\beta \approx 1670$ cm^{-1}) and libration ($r \approx 780$ cm^{-1}) vibrations also stand out in the spectrum. The ν_a-NCO band, with its characteristic quadruplet structure, is clearly visible too. It is located on top of a broad H_2O absorption attributed to a combination band ($\beta + r$). The much weaker CH_3NCO bands in the 1500–1000 cm^{-1} range are still appreciable (see the right inset in Fig. 5). The weak CH_3NCO vibrational modes below 900 cm^{-1} or above 3000 cm^{-1} are blended with intense water absorptions and are not considered further. No other significant peaks are identified in the spectral region investigated, which indicates that methyl isocyanate and water do not react appreciably at 20 K, but form a stable mixture. The ν_a-NCO band profile resembles that of amorphous CH_3NCO over the 20–85 K range (see Fig. 2), but with noteworthy differences attributable to the different environments felt by the CH_3NCO molecules. In the ice mixture, the peaks are sharper and shifted towards higher frequencies, and the second and third peaks have comparable intensities. Under the deposition conditions of this experiment, the individual CH_3NCO molecules should be surrounded by water molecules within a porous ice structure (Maté, Rodríguez-Lazcano & Herrero 2012a) with an approximate bulk density of 0.65 g cm^{-3}. The peak positions for the four components of the ν_a-NCO band in different environments are listed in Table 5.

The maxima in the spectrum of the amorphous solid are redshifted by 7–9 cm^{-1} with respect to those in water ice, which are in general redshifted with respect to those in the N_2 matrix and in the vapour. This trend reflects the degree of perturbation of the molecular vibration by the surroundings. It is worth observing that the shift in frequencies between the ice, where the CH_3NCO molecules are embedded in a bulk phase of polar water molecules, and those

Table 6. Band strengths for CH_3NCO absorptions in H_2O/CH_3NCO (1.5 per cent) ice mixtures co-deposited at 20 K.

Peak (cm^{-1})	Wavelength range (cm^{-1})	Wavelength range (μm)	A' (cm molecule^{-1})	Band assignment
2305	2220–2380	4.50–4.20	1.5×10^{-16}	ν_a-NCO
1447	1435–1485	6.99–6.73	3.7×10^{-18}	δ_a-CH_3 + ν_s-NCO
1417	1393–1432	7.18–6.98	1.9×10^{-18}	δ_s-CH_3
1135	1114–1146	8.98–8.73	1.0×10^{-18}	r-CH_3

Note. The estimated uncertainties are 30 per cent for the ν_a-NCO band and 50 per cent for the rest.

in the weakly interacting non-polar N_2 matrix is smaller (<5 cm^{-1}) than those between the amorphous solid and the CH_3NCO/H_2O ice, which suggests a comparatively strong interaction between the CH_3NCO molecules in the amorphous solid.

The band strengths of methyl isocyanate in ice can be estimated from a comparison with the intense ν-OH absorption of water ice, whose band strength is well known (Mastrapa et al. 2009; Bouilloud et al. 2015). If we assume that CH_3NCO is component 1 and H_2O is component 2 in the ice mixture, the strength of band b of methyl isocyanate, $A'_{1,b}$ can be expressed as

$$A'_{1,b} = A'_{2,\,\mathrm{v(OH)}}\,\frac{N_2}{N_1}\,\frac{\int^{\tau}_{1,b}(\upsilon)\,\mathrm{d}\upsilon}{\int^{\tau}_{2,\mathrm{v(OH)}}(\upsilon)\,\mathrm{d}\upsilon} \qquad (3)$$

where $A'_{2,\,\mathrm{v(OH)}}$ is the band strength of the OH stretching mode of water ice and N_2/N_1 is the ratio of column densities in the ice. For vapour-deposited water ice at 20 K, we take $A'_{2,\,\mathrm{v(OH)}} = 1.9 \times 10^{-16}$ cm molecule^{-1} (Mastrapa et al. 2009). We also note that the column density ratio in our experiment is the same as the molecular ratio estimated for the ice: $N_2/N_1 \approx 67$. The quotient of integrated optical depths can be substituted by the corresponding quotient of integrated experimental absorbances. The band strengths derived from the present measurements are listed in Table 6.

The estimated strength of the ν_a-NCO band of methyl isocyanate in ice is ≈15 per cent higher than that of the same band in pure amorphous CH_3NCO (see Table 2), but the two values are within their mutual experimental error. The rest of the band strengths are of the same order as the corresponding ones for pure CH_3NCO ice and they also lie within their mutual uncertainties. These bands are probably too weak to be of practical use for astronomical searches.

5 ASTROPHYSICAL IMPLICATIONS

The discovery of a relatively large proportion of CH_3NCO (1.3 per cent with respect to H_2O) in the material extracted from the surface of comet 67P/CG came as a surprise to the astronomical community (Goesmann et al. 2015). At that time, this compound had not been detected anywhere in space. Although comets are subjected to a substantial re-processing in their journey through the Solar system, at least part of their components is believed to be remnants from the original molecular cloud that gave rise to the solar nebula, and that could be the case of methyl isocyanate. Shortly after its detection in comet 67P/CG, methyl isocyanate was identified in the gas phase of hot cores in Sgr B2 and Orion (Halfen, Ilyushin & Ziurys 2015; Cernicharo et al. 2016). It is believed that the molecule is formed in the ices of molecular clouds and then released from the grains in the transition to the hot core phase (Cernicharo et al. 2016). The estimated CH_3NCO/H_2O ratio (≈0.02 per cent) in hot cores is much lower than that of comet 67P/CG, which suggests that part of the methyl isocyanate in the hypothetic original ices may remain in the solid phase during cloud collapse and be incorporated to cold bodies in planetary systems.

The obvious spectroscopic feature for a search of CH_3NCO in interstellar ices is the intense ν_a-NCO band at ≈2220–2350 cm^{-1} (4.25–4.50 μm) discussed throughout this work. This frequency interval is not adequate for observations from Earth since it partly overlaps with the lower frequency wing of the atmospheric CO_2 absorption at ≈2349 cm^{-1} (4.26 μm). Data from space-based observatories have become available over the last decades both for massive young stellar objects (YSOs) (Gibb et al. 2004; Dartois 2005) and low-mass YSOs (Boogert et al. 2008; Oberg et al. 2011; Boogert, Gerakines & Whittet 2015). In interstellar ices, the strong absorption of CO_2 at 2341 cm^{-1} can interfere somewhat with the ν_a-NCO band of CH_3NCO. However, the mentioned CO_2 absorption is narrow and for typical CO_2 ice concentrations (Boogert, Gerakines & Whittet 2015) the perturbation should be limited to the high-frequency edge of the methyl isocyanate band. The Solar system evolved from a low-mass YSO and it is likely that its primeval ices resembled those that are in this type of objects. An extensive survey of ices in low-mass YSOs was performed in the course of the *Spitzer* mission (Oberg et al. 2011), but these observations were limited to wavenumbers lower than 2000 cm^{-1} ($\lambda > 5$ μm) and thus do not cover the region of interest here. The 2220–2350 cm^{-1} (4.25–4.50 μm) spectral interval was actually included in the previous study of a smaller sample of massive YSOs carried out with the *Infrared Space Observatory* (*ISO*; Gibb et al. 2004; Dartois 2005), but the molecule was not identified. Ices around massive YSOs often show a band at ≈2165 cm^{-1} (4.62 μm), attributed to OCN^- (Hudson, Moore & Gerakines 2001; van Broekhuizen et al. 2005; Maté et al. 2012b), which is taken as a signature of the strong ice processing typical for these objects (Boogert, Gerakines & Whittet 2015) and could be chemically related to isocyanic acid and isocyanates. In fact, Hudson, Moore & Gerakines (2001) have shown that electron bombardment of $C_2H_5NCO + H_2O$ ice mixtures leads to the appearance of this OCN^- absorption feature probably through a mechanism of dissociative electron attachment. The ν_a-NCO band of methyl isocyanate should appear between this band and the intense band of CO_2 in ice at 4.27 μm. In this region, only a small peak at 4.38 μm, attributed to ^{13}CO, has been confidently identified (Boogert, Gerakines & Whittet 2015). A faint multipeak structure is insinuated in some of the *ISO* spectra between the two prominent absorptions at 4.25 and 4.62 μm (Boogert et al. 2000), but the signal-to-noise ratio is too low and the band analysis too complex to draw any conclusion on the presence of other species. A detailed investigation of this region in low-mass YSOs would be worthwhile since they are more representative of the early Solar system. As discussed by Boogert et al. (2008) in their thorough analysis of *Spitzer* data, the identification of minor ice species in the IR spectra is a complex task due to the concurrence of many possible carriers with the consequent overlapping of spectral bands in the naturally

weak absorption features. In this respect, methyl isocyanate may be an exception. The high CH_3NCO/H_2O ratio reported for comet 67P/CG, and the characteristic multiplet structure of its intense ν_a-NCO band, which is constrained between well-known CO_2 and XCN absorptions, makes it a very good candidate for searches with the new generation of high-resolution upcoming facilities like the *James Webb Space Telescope*.

6 CONCLUSIONS

After the discovery of methyl isocyanate on comet 67P/Churyumov–Gerasimenko, this molecule has become the target of several astrophysical studies. We present here new results based on laboratory and theoretical investigations. The main conclusions are given below.

The spectra of CH_3NCO present several interesting features. The most outstanding is a strong, complex band at $\sim$2300 cm^{-1}, assigned to the asymmetric stretch of the NCO backbone. It has four components whose origin is not yet fully understood. The structure of this zone is maintained upon warming up to 85 K, but it shows wavenumber shifts and rearrangements when methyl isocyanate is mixed with water, in an N_2 matrix, or in the gas phase. Thus, this feature could reveal interesting information on the nature and surroundings of CH_3NCO if detected in the ice form in astrophysical media other than comets.

The evolution of the spectra with temperature allows observing a phase change from amorphous to crystalline at 90 K. Besides the usual sharpening of IR bands, some wavenumber shifts take place associated with this phase transition, especially again in the NCO band.

This vibration is also strong in the spectrum of CD_3NCO, in the same wavenumber region, but with a slightly different pattern. Further studies on this subject would be highly interesting.

The crystalline structure of CH_3NCO was not known. We have derived a tentative structure based on that of isocyanic acid, HNCO, for which some information was available. The results of the model seem acceptable concerning the structure of the unit cell, the bonding among the four enclosed molecules and the predicted IR spectrum.

For astrophysical purposes, band strengths are of key importance. We have measured these values for the spectra of CH_3NCO and CH_3NCO/H_2O ices at 20 K. Good agreement is obtained with the scarce previous information on these data.

Analysis of the spectrum of CH_3NCO/H_2O ice at 20 K does not disclose any features indicative of the formation of new species. Therefore, although CH_3NCO reacts with H_2O at higher temperatures, it seems to form a stable mixture at 20 K.

ACKNOWLEDGEMENTS

We are indebted to P. C. Gómez, M. L. Senent and M. A. Moreno for helpful discussions. This work was funded by the European Union under grant ERC-2013-Syg 610256 (NANOCOSMOS) and by the Spanish MINECO CSD2009-00038 (ASTROMOL) within the Consolider–Ingenio Program. MINECO funding from grants FIS2013-48087-C2-1P, FIS2016-C3-1P, AYA2012-32032 and AYA2016-75066-C2-1-P is also acknowledged. G. M. acknowledges MINECO PhD grant BES-2014-0693. JCG and JC also thank the ANR-13-BS05-0008 IMOLABS and JCG thanks the Program PCMI (INSU-CNRS) and the Centre National d'Etudes Spatiales (CNES) for funding support.

REFERENCES

Anderson D. W., Rankin D. W. H., Robertson A., 1972, J. Mol. Struct., 14, 385
Boogert A. C. A. et al., 2000, A&A, 353, 349
Boogert A. C. A., Gerakines P. A., Whittet D. C. B., 2015, ARA&A, 53, 541
Boogert A. C. A. et al., 2008, ApJ, 678, 985
Bouilloud M., Fray N., Bénilan Y., Cottin H., Gazeau M. C., Jolly A., 2015, MNRAS, 451, 2145
Cernicharo J. et al., 2016, A&A, 587, L4
Clark S. J., Segall M. D., Pickard C. J., Hasnip P. J., Probert M. J., Refson K., Payne M. C., 2005, Z. Kristallogr., 220, 567
Curl R. S., Sasty K. V. L., Rao V. L., Hodgeson J. A., 1963, J. Chem. Phys., 39, 3335
Dalbouha S., Senent M. L., Komiha N., Domíngez-Gómez R., 2016, J. Chem. Phys., 145, 124309
Dartois E., 2005, Space Sci. Rev., 119, 293
D´Hendecourt L. B., Allamandola L. J., 1986, ApJS, 64, 453
D´Silva T. D. J., Lopes A., Jones R. L., Singhagwangcha S., Chan J. K., 1986, J. Org. Chem., 51, 3781
Eyster E. H., Gillette R. H., Brockway L. O., 1940, J. Am. Chem. Soc., 62, 3236
Fernández-Martínez A., Timon V., Roman-Ross G., Cuello G. J., Daniels J. E., Ayora C., 2010, Am. Mineral., 95, 1312
Gálvez O., Maté B., Herrero V. J., Escribano R., 2008, Icarus, 197, 599
Gerakines P. A., Schutte W. A., Greenberg J. M., van Dishoeck E. F., 1995, A&A, 296, 810
Gibb E. L., Whittet D. C. B., Boogert A. C. A., Tielens A. G. G. M., 2004, ApJS, 151, 35
Goesmann F. et al., 2015, Science, 349, aab0689
Grimme S., 2006, J. Comput. Chem., 27, 1787
Halfen D. T., Ilyushin V. V., Ziurys L. M., 2015, ApJ, 812, L5
Han D. H., Pearson P. G., Baillie T. A. J., 1989, J. Labelled Compd. Radiopharmaceuticals, 27, 1371
Herbst E., van Dishoeck E. F., 2009, ARA&A, 47, 427
Hirschmann R. P., Kniseley R. N., Fassel V. A., 1965, Spectrochim. Acta, 21, 2125
Hudson R. L., Moore M. H., Gerakines P. A., 2001, ApJ, 550, 1140
Hudson R. L., Ferrante R. F., Moore M. H., 2014, Icarus, 228, 276
Hwang W., Kim Y. K., Rudd M. E., 1996, J. Chem. Phys., 104, 2956
Kasten W., Dreizler H., 1986, Z. Nat. forsch. A, 41, 637
Koput J., 1984, J. Mol. Spectrosc., 106, 12
Koput J., 1986, J. Mol. Spectrosc., 115, 131
Koput J., 1988, J. Mol. Spectrosc., 127, 51
Lett R. G., Flygare W. H., 1967, J. Chem. Phys., 47, 4730
Lowenthal M. S., Khanna R. K., Moore M. H., 2002, Spect rochim. Acta, 58, 73
Martín-Doménech R., Manzano-Santamaría J., Muñoz Caro G. M., Cruz-Díaz G. A., Chen Y.-J., Herrero V. J., Tanarro I., 2015, A&A, 584, A14
Mastrapa R. M., Sandford S. A., Roush T. L., Cruikshank D. P., D'Alle Ore C. M., 2009, ApJ, 701, 1347
Maté B., Medialdea A., Moreno M. A., Escribano R., Herrero V. J., 2003, J. Chem. Phys. B, 107, 11098
Maté B., Rodríguez-Lazcano Y., Herrero V. J., 2012a, Phys. Chem. Chem. Phys., 14, 10595
Maté B., Herrero V. J., Rodríguez-Lazcano Y., Fernández-Torre D., Moreno M. A., Gómez P. C., Escribano R., 2012b, ApJ, 759, 90
Maté B., Tanarro I., Moreno M. A., Jiménez-Redondo M., Escribano R., Herrero V. J., 2014, Faraday Discuss., 168, 267
Oberg K. I., Boogert A. C. A., Pontoppidan K. M., van den B. S., van D. E. F., Bottinelli S., Blake G. A., Evans N. J., II, 2011, ApJ, 740, 109
Ozaki S., 1972, Chem. Rev., 72, 458
Perdew J. P., Burke K., Ernzerhof M., 1996, Phys. Rev. Lett., 77, 3865
Refson K., Tulip P. R., Clark S. J., 2006, Phys. Rev. B, 73, 155114
Reva I., Lapinski L., Fausto R., 2010, J. Mol. Spectrosc., 976, 333
Saunders J. H., Slocombe R. J., 1948, Chem. Rev., 43, 203

Sullivan J. F., Heusel H. L., Zunic W. M., Durig J. R., 1994, Spectrochim. Acta, 50A, 435
Teles J. H., Maier G., Hess B. A., Schaad L. J., Winnewisser M., Winnewisser B. P. 1989, Chem. Ber., 122, 753
van Broekhuizen F. A., Pontoppidan K. M., Frazer K. M., van Dishoeck E. F., 2005, A&A, 441, 249
von Dohlen W. C., Carpenter G. B., 1955, Acta Crystallogr., 8, 646
Zhou S. X., Durig J. R., 2009, J. Mol. Spectrosc., 924, 111

CALIBRATION OF THE QUADRUPOLE MASS SPECTROMETER

For the calibration of the QMS, we measured the intense OH absorption band between 4939 and 2969 cm^{-1} of water ice deposited at 20 K. The column density, N_{H2O}, of water molecules in the ice is given by

$$N_{H2O} = \frac{1}{A'_{H2O}} \int \tau(\upsilon)\, d\upsilon \quad \text{(A1)}$$

where A'_{H2O} is the band strength of the OH band and $\tau(\nu)$ is the optical depth at frequency ν. If we assume a sticking probability of one for water molecules hitting the substrate at 20 K, the column density can be expressed as

$$N_{H2O} = z \times \Delta t \quad \text{(A2)}$$

where z is the frequency of surface collisions and Δt is the deposition time. The molecular collision frequency with a wall is given by

$$z = n_{H2O}\langle v\rangle = n_{H2O}\left(\frac{kT}{2\pi m}\right)^{1/2} \quad \text{(A3)}$$

where n_{H2O} is the molecular density, held constant during deposition, and $\langle v\rangle$ is the average velocity of the colliding molecules, which can be expressed in terms of the gas temperature, T, the Boltzmann constant, k, and the molecular mass m. The molecular density of H_2O is readily derived as

$$n_{H2O} = \frac{\int \tau(\upsilon)\, d\upsilon}{A'_{OH}\Delta t}\left(\frac{kT}{2\pi m}\right)^{-\frac{1}{2}} \quad \text{(A4)}$$

The integral can be obtained from the measured integrated absorbance over the frequency range of interest and the band strength is taken from the literature $A'_{OH} = 1.9 \times 10^{-16}$ cm molecule^{-1} (Mastrapa et al. 2009). The QMS signal corresponding to mass 18 can be expressed as $I_{18} = c \times n_{H2O}$, where c is a proportionality constant.

For the calibration of the QMS for methyl isocyanate, we used H_2O as reference. The different detection efficiencies for the two species were corrected by taking into account the dependence of the QMS signals, I_i, on the ionization cross-section and fragmentation pattern (Martín-Doménech et al. 2015):

$$I_i \propto n_m \sigma_m f_i \quad \text{(A5)}$$

where I_i is the QMS reading for peak i from species m, n_m is the molecular density of species m, σ_m its electron impact ionization cross-section and f_i is the fraction of the total m signal corresponding to peak i. Using the peak of mass 57 for CH_3NCO, the molecular density in the deposition chamber is given by

$$n_{CH3NCO} = \frac{I_{57} \times n_{H2O} \times \sigma_{H2O} \times f_{18}}{I_{18} \times \sigma_{CH3NCO} \times f_{57}} \quad \text{(A6)}$$

Equation (A6) tacitly assumes that the detection sensitivity is roughly the same for the two mass fragments, which is the case for the QMS used. The cross-sections $\sigma_{H2O} = 2.53$ Å^2 and $\sigma_{CH3NCO} = 7.55$ Å^2 were taken from table S4 of Goesmann et al. (2015). These values were calculated for an electron energy of 70 eV (as employed in the QMS) with the Binary–Encounter–Bethe (BEB) model (Hwang, Kim & Rudd 1996). We also used $f_{18} = 0.81$ and $f_{57} = 0.44$ derived from the respective QMS electron impact fragmentation patterns of water and methyl isocyanate. From this equation, a calibration constant c' can be derived for methyl isocyanate: $I_{57} = c' \times n_{CH3NCO}$.

There are several sources of error associated with the calibration procedure just described (assumed sticking coefficient, pressure fluctuations during deposition, ionization cross-section values, etc.), which are difficult to assess precisely. We assume a conservative 30 per cent uncertainty for the n_{CH3NCO} values derived with this procedure.

This paper has been typeset from a Microsoft Word file prepared by the author.